Supplementary material

Modeling Diurnal Variation of SOA Formation via Multiphase Reactions of Biogenic Hydrocarbons

Sanghee Han and Myoseon Jang*
Department of Environmental Engineering Science, University of Florida, Gainesville, Florida, USA

Correspondence to: Myoseon Jang (mjang@ufl.edu)

This file includes:
6 Sections
1 Table
4 Figures
4 Schemes
References

Section S1. The oxidation process of biogenic hydrocarbons.

Section S1.1 Gas mechanism in SAPRC07tic

In this study, the oxidation of biogenic hydrocarbons (isoprene, α-pinene, and β-caryophyllene) was simulated by using SAPRC07tc. In the mechanism, the biogenic hydrocarbons are oxidized by 4 major oxidants (OH radicals, O_3, NO_3 radicals, and $O(^3P)$). The reaction rate constants of β-caryophyllene were determined based on the MCM v3.3.1 (Jenkin et al., 2012) and reduced to simulate the oxidation of β-caryophyllene in the chamber.

Table S1. The oxidation mechanisms of isoprene, α-pinene, and β-caryophyllene in this study.

ID	Reaction	Rate constant (molecule s^{-1})
ISOP1	ISOP + O3P = 0.25*MEO2 + 0.24*XMA3 + 0.24*RO2C + 0.01*RO2X + 0.01*ZRN3 + 0.24*XHCH +0.75*PRD2 + 0.25*Y6PX - 1.01*XC	3.5×10^{-11}
ISOP2	ISOP + OH = 0.907*XHO2 + 0.986*RO2C + 0.093*RO2X + 0.093*ZRN3 + 0.624*XHCH + 0.23*XMAC + 0.32*XMVK + 0.357*XIPR + Y6PX -0.167*X	$2.54\times 10^{-11} \times e^{\frac{410}{T}}$
ISOP3	ISOP + O3 = 0.066*HO2 + 0.266*OH + 0.192*XMA3 + 0.192*RO2C + 0.008*RO2X + 0.008*ZRN3 + 0.275*CO + 0.122*CO2 + 0.4*HCHO +0.192*XHCH + 0.204*FACD + 0.39*MACR + 0.16*MVK + 0.15*IPRD + 0.1*PRD2 + 0.2*Y6PX -0.559*XC	$7.86\times 10^{-15} \times e^{\frac{-1912}{T}}$
ISOP4	ISOP + NO3 = 0.749*XHO2 + 0.187*XNO2 + 0.936*RO2C + 0.064*RO2X + 0.064*ZRN3 +0.936*XIPR + Y6PX + 0.813*XN - 0.064*XC	$3.03\times 10^{-12} \times e^{\frac{-448}{T}}$
APIN1	APIN + O3P = PRD2 + 4*XC	3.20×10^{-11}
APIN2	APIN + OH = 0.799*XHO2 + 0.004*XRC3 + 1.042*RO2C + 0.197*RO2X + 0.197*ZRN3 + 0.002*XCO+ 0.022*XHCH + 0.776*XRCH + 0.034*XACE +0.02*XMGL + 0.023*XBAC + Y6PX + 6.2*XC	$1.21\times 10^{-11} \times e^{\frac{436}{T}}$
APIN3	APIN + O3 = 0.009*HO2 + 0.102*XHO2 + 0.728*OH + 0.001*XMC3 + 0.297*XRC3 + 1.511*RO2C+ 0.337*RO2X + 0.337*ZRN3 + 0.029*CO +0.051*XCO + 0.017*CO2 + 0.344*XHCH + 0.24*XRCH + 0.345*XACE + 0.008*MEK + 0.002*XGLY+ 0.081*XBAC + 0.255*PRD2 + 0.737*Y6PX +2.999*XC	$5.00\times 10^{-16} \times e^{\frac{-530}{T}}$
APIN4	APIN + NO3 = 0.056*XHO2 + 0.643*XNO2 +0.007*XRC3 + 1.05*RO2C + 0.293*RO2X + 0.293*ZRN3 + 0.005*XCO + 0.007*XHCH + 0.684*XRCH+ 0.069*XACE + 0.002*XMGL + 0.056*XRN3 + Y6PX + 0.301*XN + 5.608*XC	$1.19\times 10^{-12} \times e^{\frac{490}{T}}$
SESQ1	SESQ + O3P = 0.237*RCHO + 0.763*PRD2 + 9.711*XC	4.02×10^{-11}
SESQ2	SESQ + OH = 0.734*XHO2 + 0.064*XRC3 + 1.211*RO2C + 0.201*RO2X + 0.201*ZRN3 +0.001*XCO + 0.411*XHCH + 0.385*XRCH +0.037*XACE + 0.007*XMEK + 0.003*XMGL +0.009*XBAC + 0.003*XMVK + 0.002*XIPR + 0.409*XPD2 + Y6PX + 9.375*XC	1.97×10^{-12}
SESQ3	SESQ + O3 = 0.078*HO2 + 0.046*XHO2 + 0.499*OH + 0.202*XMC3 + 0.059*XRC3 + 0.49*RO2C + 0.121*RO2X + 0.121*ZRN3 + 0.249*CO + 0.063*CO2 + 0.127*HCHO + 0.033*XHCH + 0.208*XRCH + 0.057*XACE + 0.002*MEK + 0.172*FACD+ 0.068*PACD + 0.003*XMGL + 0.039*XBAC +0.002*XMAC + 0.001*XIPR + 0.502*PRD2 +0.428*Y6PX + 8.852*XC	1.8×10^{-15}
SESQ4	SESQ + NO3 = 0.227*XHO2 + 0.287*XNO2 +0.026*XRC3 + 1.786*RO2C + 0.46*RO2X + 0.46*ZRN3 + 0.012*XCO + 0.023*XHCH + 0.002*XCCH+ 0.403*XRCH + 0.239*XACE + 0.005*XMAC +0.001*XMVK + 0.004*XIPR + 0.228*XRN3 +Y6PX + 0.485*XN + 8.785*XC	1.90×10^{-11}

Section S1.2 Additional gas oxidation paths to the explicit gas mechanism

The gas-phase oxidation of three biogenic HCs (isoprene, α-pinene, and β-caryophyllene) of this study was explicitly processed by using the Master Chemical Mechanism (MCM v3.3.1) (Saunders et al., 2003;Jenkin et al., 2012;Jenkin et al., 2015) to generate lumping species and their model parameters. The recently identified oxidation mechanisms that can yield low volatile products were also integrated with MCM. For example, the Peroxy Radical Autoxidation Mechanism (PRAM) (Roldin et al., 2019) that forms the highly oxygenated organic molecule (HOM) (Molteni et al., 2019) and the accretion reaction to form ROOR from the RO_2 (Bates et al., 2022;Zhao et al., 2021) were added. Furthermore, the oxidation process of biogenic HCs by $O(^3P)$ (Paulson et al., 1992;Alvarado et al., 1998) was included in gas mechanisms to fulfill the oxidation mechanism used in the current regional model.

The accretion reaction to form ROOR from the NO_3-originated RO_2 from α-pinene has been reported by (Bates et al., 2022;Zhao et al., 2021). Thus, the ROOR formation of NO_3-originated RO_2 from all three HCs were applied as presented in Schemes S1-S3. The oxidation of isoprene with $O(^3P)$ is shown in Scheme S4 as an example.

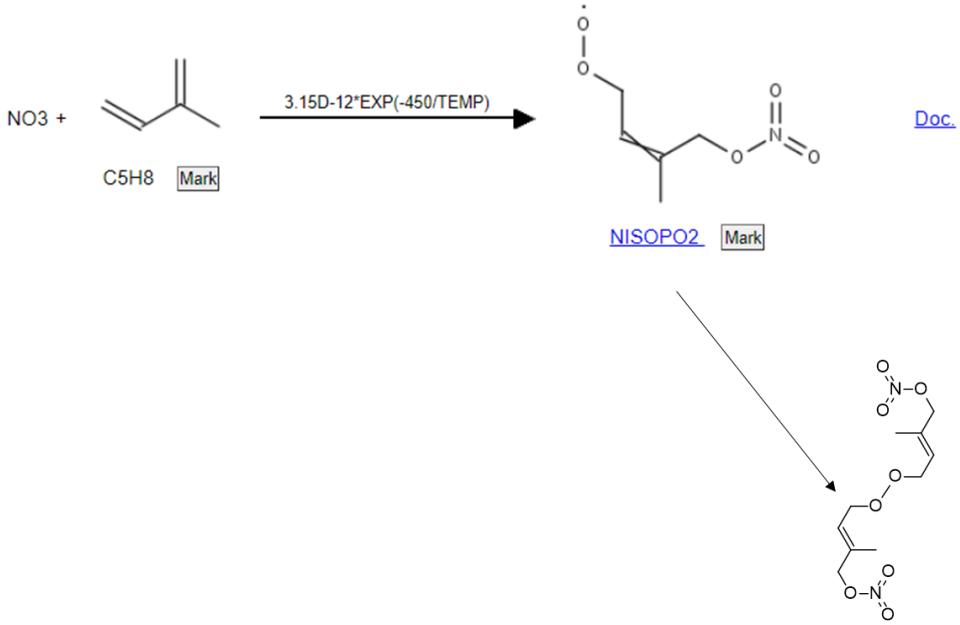

Scheme S1. The ROOR formation process of the NO_3-originated RO_2 from isoprene.

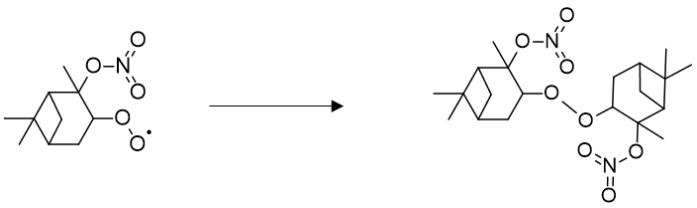

Scheme S2. The ROOR formation process of the NO_3-originated RO_2 from α-pinene.

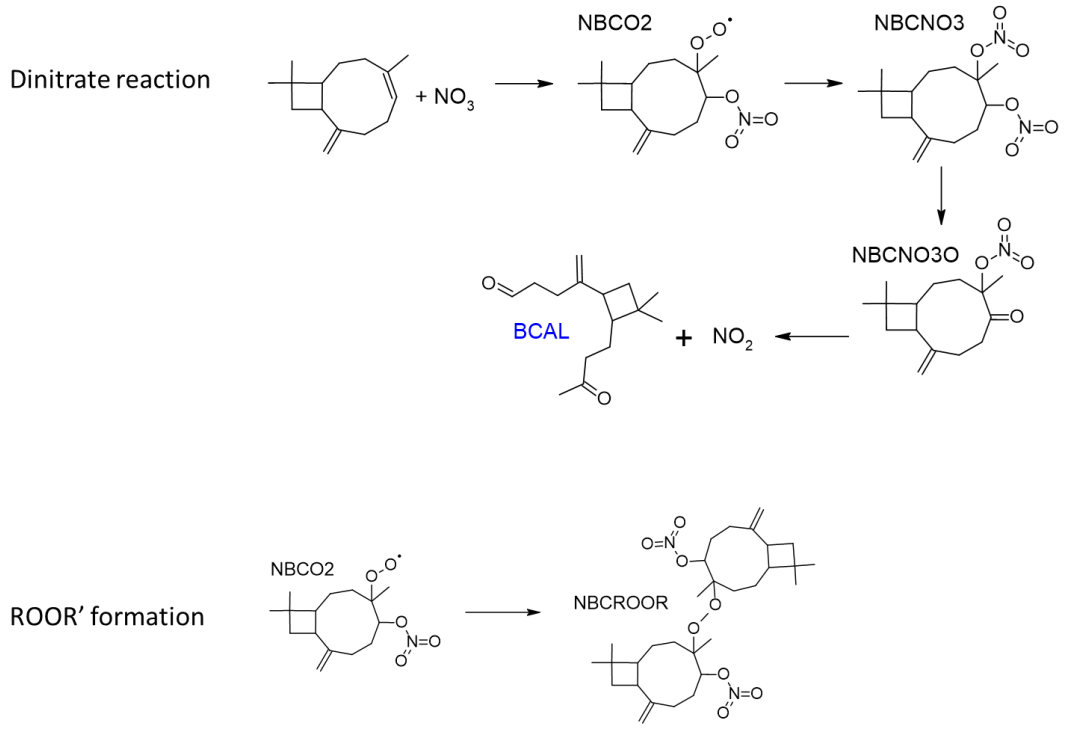

Scheme S3. The dinitrate formation in β-caryophyllene and the further reaction to form ROOR.

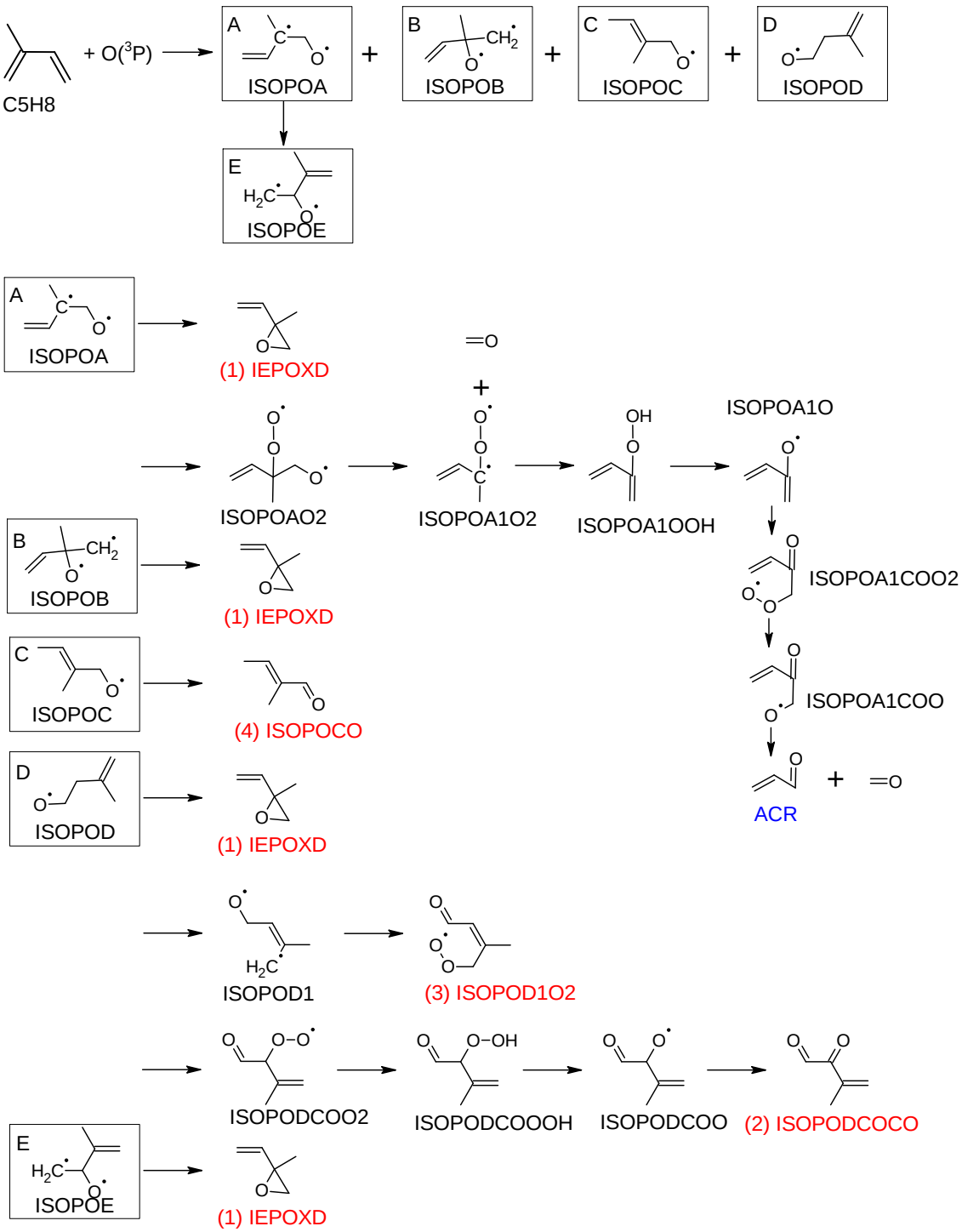

Scheme S4. Isoprene oxidation path by O(^{3}P) (continue).

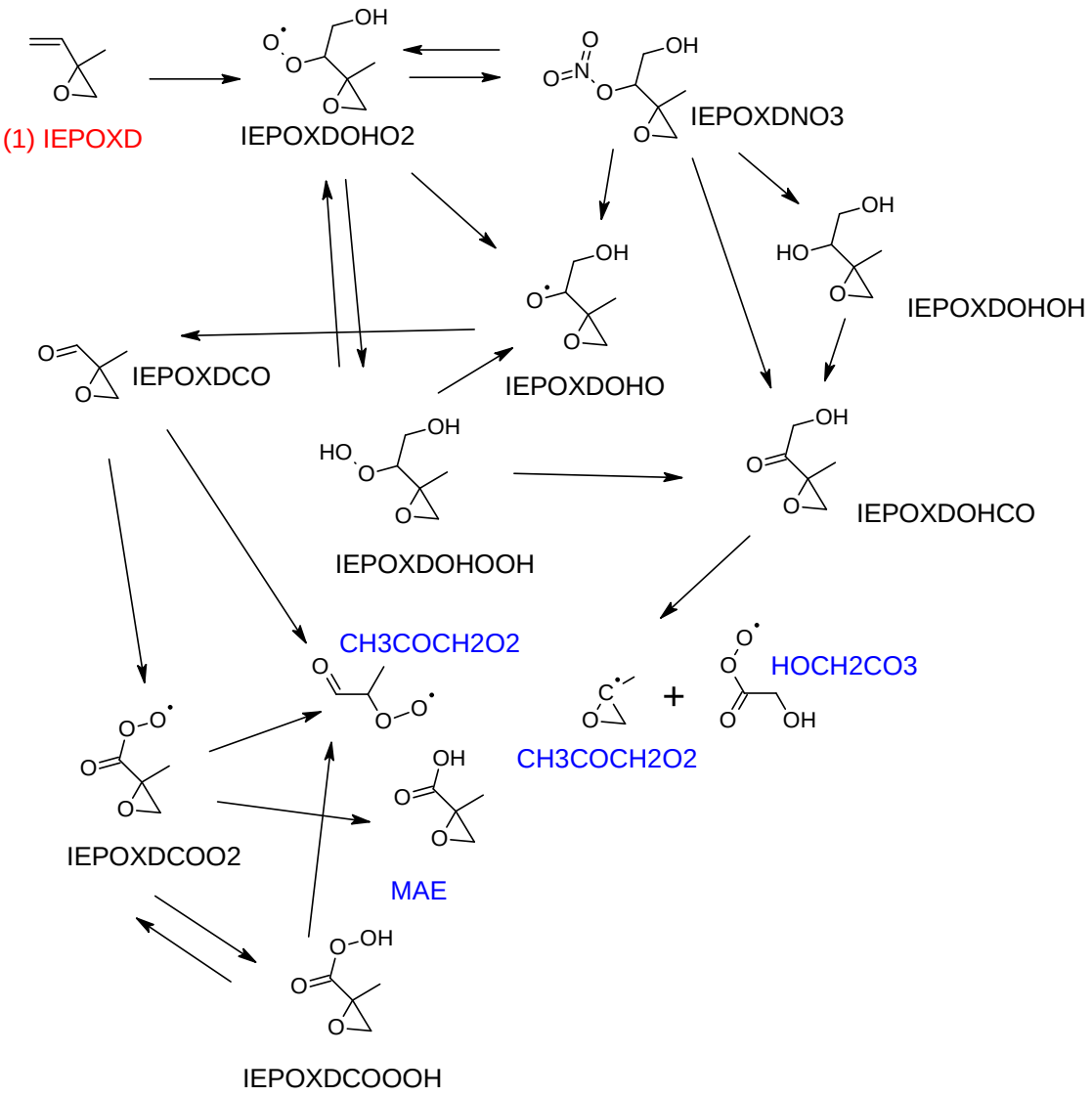

Scheme S4. Isoprene oxidation path by O(^{3}P) (continue).

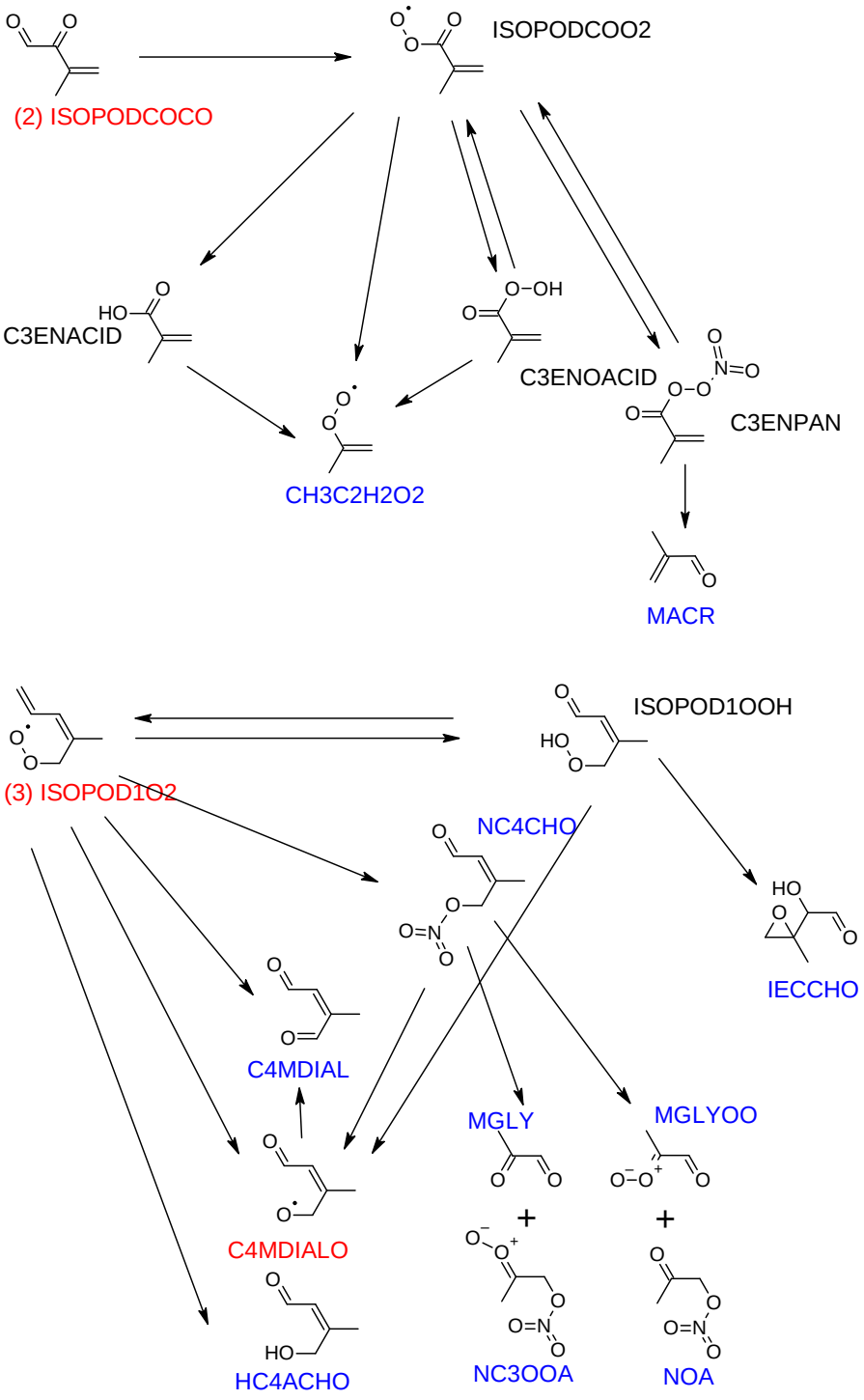

Scheme S4. Isoprene oxidation path by O(^{3}P) (continue).

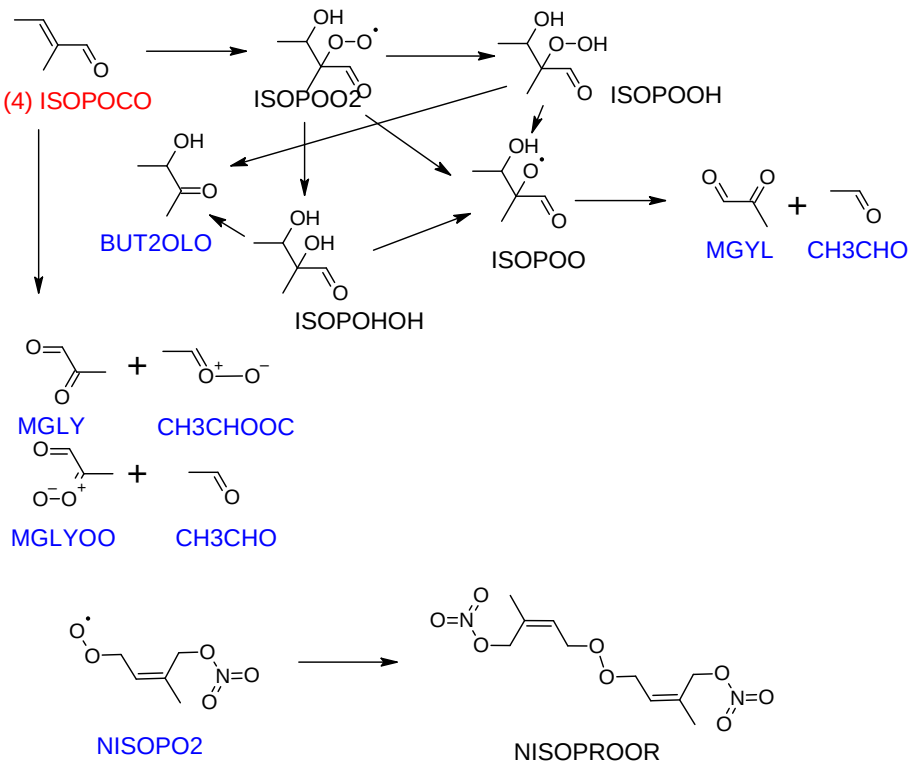

Scheme S4. Isoprene oxidation path by O(^{3}P).

Section S2. Reference conditions for the simulation.

The sunlight intensity illustrated in Fig. S1 was measured on 06/19/2015 in the UF-APHOR and is applied as a reference sunlight intensity for the sensitivity and uncertainty tests. The daytime SOA formation in Figs. 5 and 6 were simulated at a given reference condition, to investigate the diurnal variations in biogenic SOA and the sensitivity of temperature and the NO_x levels to the biogenic SOA from each oxidation path.

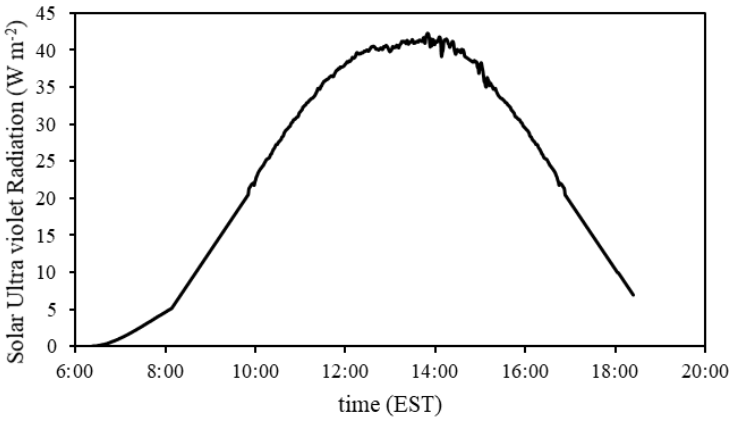

Figure S1. Time profiles of reference sunlight radiance measured by using Total Ultra-Violet Radiation (TUVR) in the UF-APHOR on 06/19/2015.

Section S3. The contribution of each oxidation path to the hydrocarbon consumption

In Figs. 5 and 6, the gas oxidation was simulated under the two different NO_x conditions at the given reference condition. Figure S2 illustrates the contribution of each oxidant to the total biogenic HC consumption suggesting the importance of each oxidation path at day and night.

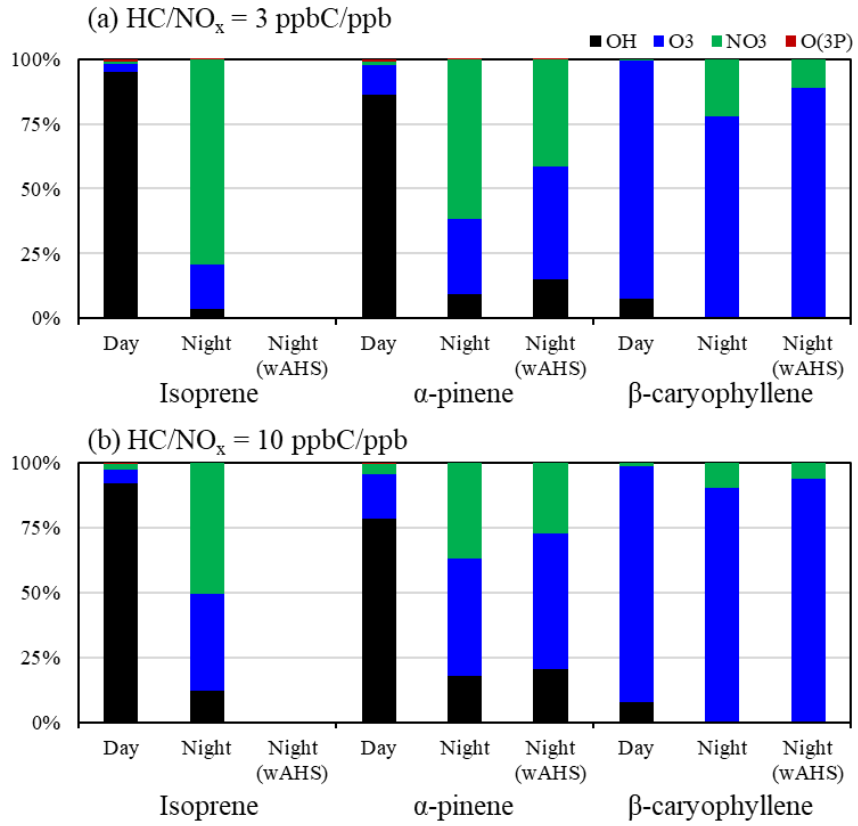

Figure S2. The contribution of each oxidation path on the consumption of isoprene, α–pinene, and β-caryophyllene at the given condition under three different NO_x level ((a) HC/NO_x = 3 ppbC/ppb and (b) HC/NO_x = 10 ppbC/ppb). The gas oxidation in daytime was simulated under the reference sunlight intensity which is measured on 06/19/2015 (Fig. S1).

Section S4. Wall-free biogenic SOA formation

The chamber-generated SOA mass is influenced by the deposition of organic vapor to the chamber wall. The simulation of SOA yields in Fig. 4 is performed with the model parameters obtained in the presence of the chamber wall. To investigate the SOA formation in the ambient air, the wall-free SOA model parameter has recently been derived by (Han and Jang, 2022). Figure S3 displays the potential SOA yield without the chamber wall bias simulated by the UNIPAR-SAPRC model from each oxidation path, which is calculated with the same amount of HC consumption at two different NO_x levels ((a) high NO_x: HC/NO_x = 3 ppbC/ppb and (b) low NO_x: HC/NO_x = 10 ppbC/ppb). For this calculation, the consumptions of biogenic HCs are set to 50 ppb (138 μg m^{-3}), 30 ppb (162 μg m^{-3}), and 20 ppb (167 μg m^{-3}) for isoprene, α-pinene, and β-caryophyllene, respectively. The temperature is set to 298 K at two different relative humidity (RH) levels (45% and 80%) and three different seed conditions (no seed, wet-AS, and wet ammonium bisulfate (AHS)) with 10 μg m^{-3} of OM_0. For the inorganic seeded simulation, the seed concentration is 20 μg m^{-3} (dry mass). The α-pinene SOA is the most influenced biogenic SOA by gas-wall partitioning, especially in the OH- and NO_3-initiated oxidation paths. The acidic seed effects on biogenic SOA formation reduce by correction of model parameters.

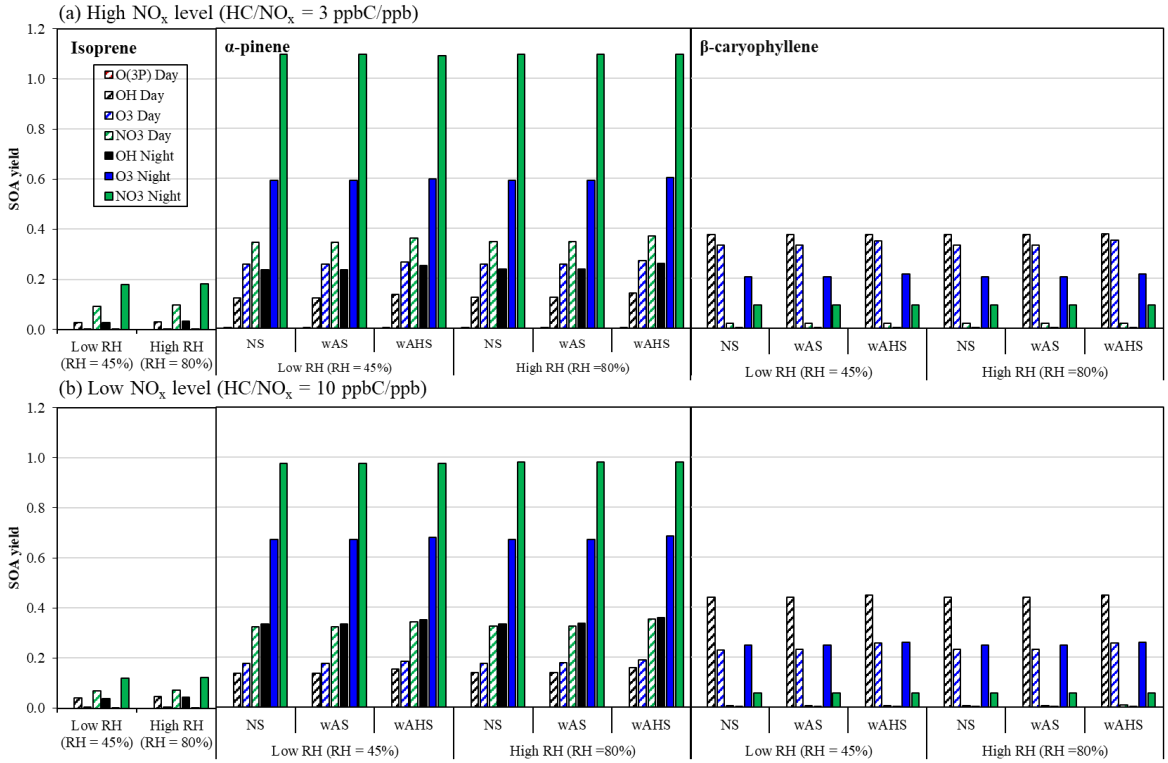

Figure S3. The potential SOA yield from each oxidation path from the given HC consumption under (a) high NO_x level (HC/NO_x = 3 ppbC/ppb) and (b) low NO_x level (HC/NO_x = 10 ppbC/ppb) in the absence of gas-wall partitioning bias. The consumption of biogenic HC was set to 50 ppb (138 μg m^{-3}), 30 ppb (162 μg m^{-3}), and 20 ppb (167 μg m^{-3}) for isoprene, α-pinene, and β-caryophyllene, respectively. The SOA formation was simulated at 298K under two different RH (45% and 80%) with 10 μg m^{-3} of OM_0. For the α-pinene and β-caryophyllene, the SOA formed at 3 different seed conditions (NS, wAS, wAHS). The wall-free model parameters were applied to simulate SOA formation (Han and Jang, 2022).

Section S5. Nighttime Biogenic SOA formation in the presence of gasoline fuel

To investigate the SOA formation in urban area, α-pinene SOA formation was simulated in the presence of gasoline fuel under three different NO_x levels (O_3 only, low NO_x (HC/NO_x = 10 ppbC/ppb), and high NO_x (HC/NO_x = 3 ppbC/ppb)) and seed conditions (NS, wet-AS, and wet-AHS). Figure S3 illustrates the simulated total SOA mass (bar) and the contribution of α-pinene SOA to the total SOA. Overall, the nighttime SOA was dominantly generated from the α-pinene with the high contributions (> 90%).

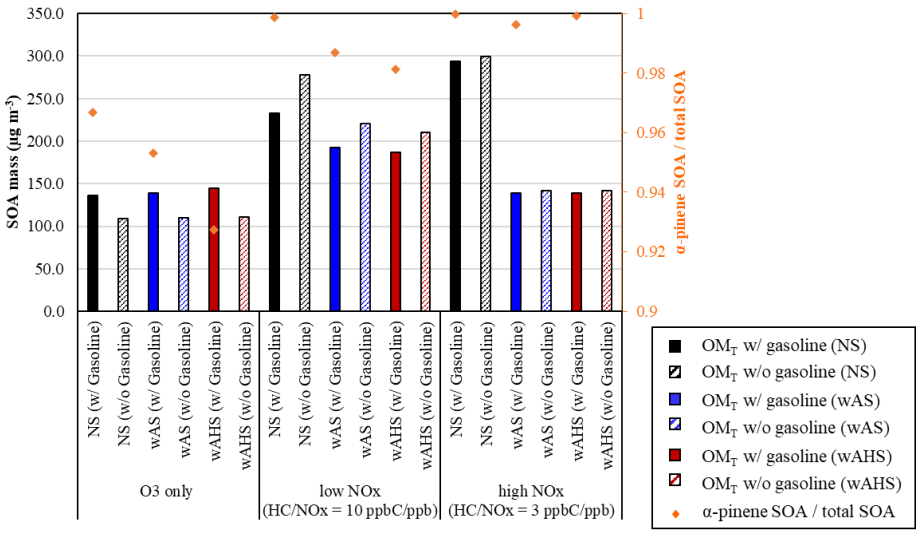

Figure S4. The α-pinene SOA mass under three different seed conditions (NS, wAS, and wAHS) and three different NO_x conditions: O_3 only, low NO_x (HC/NO_x = 10 ppbC/ppb), and high NO_x (HC/NO_x = 3 ppbC/ppb) with 10 μg m^{-3} of OM_0. To investigate the impact of the anthropogenic HCs on the oxidation and SOA formation of α-pinene, the α-pinene SOA formation was simulated with and without gasoline fuel in the system. The symbols denote the contribution of α-pinene SOA to the total SOA. The wall-free model parameters were applied to simulate SOA mass (Han and Jang, 2022).

Section S6. Uncertainties in biogenic SOA associated with the model parameters

The uncertainty test of SOA mass was performed for two major processes associated with partitioning (P_L) and aerosol phase reactions in both the organic phase and the aqueous phase (k_o, and k_{AC}) The uncertainty in SOA mass in Figure S5 was performed by increasing/decreasing P_L, k_o, and k_{AC} as a factor of 1.5/0.5, at the high NO_x level (HC/NO_x = 3 ppbC/ppb) with 10 μg m^{-3} of OM_0. The daytime SOA mass was simulated with the sunlight profile on 06/19/2015 near summer solstice. Temperature and RH set as 298K and 40%, respectively. The amount of both neutral (wet-AS) and acidic (wet-AHS) seed was fixed to 20 μg m^{-3} (dry mass).

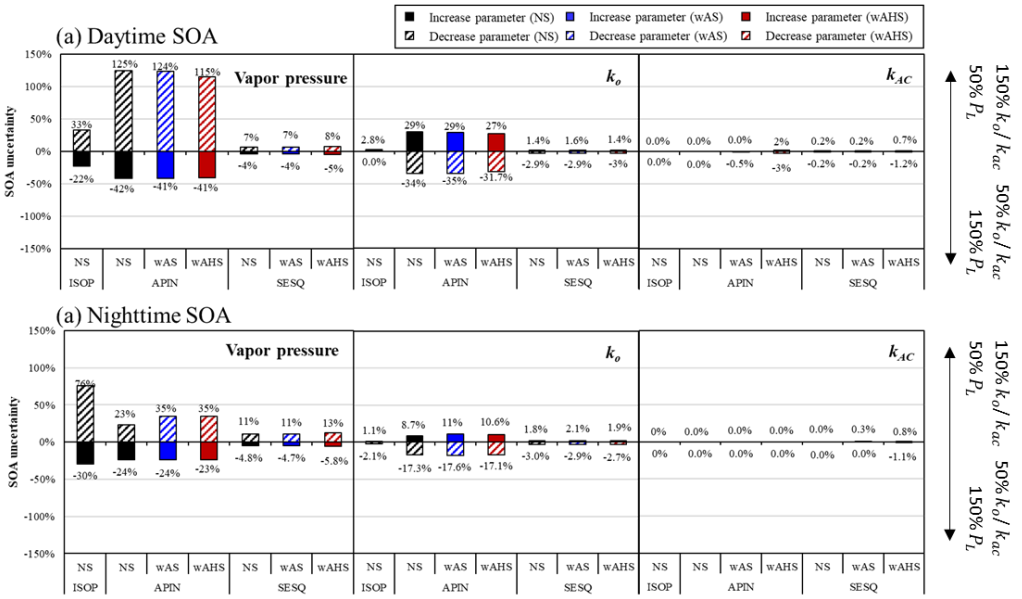

Figure S5. Uncertainties in the prediction of SOA formation associated with vapor pressure (P_L), reaction rate constant in the organic phase (k_o), and reaction rate constant in the inorganic phase (k_{AC}) in (a) day and (b) night. The simulation performed at the high NO_x level (HC/NO_x = 3 ppbC/ppb) with 10 μg m^{-3} of OM_0. The daytime SOA mass was simulated with the sunlight profile on 06/19/2015 near summer solstice (Fig. S1). Temperature and RH are set as 298K and 40%, respectively. The amount of both wet-AS and wet-AHS was fixed to 20 μg m^{-3} (dry mass). The wall-free model parameters were applied to simulate SOA mass (Han and Jang, 2022).

References

Alvarado, A., Tuazon, E. C., Aschmann, S. M., Atkinson, R., and Arey, J.: Products of the gas-phase reactions of O (3 P) atoms and O3 with α-pinene and 1, 2-dimethyl-1-cyclohexene, Journal of Geophysical Research: Atmospheres, 103, 25541-25551, 1998.

Bates, K. H., Burke, G. J., Cope, J. D., and Nguyen, T. B.: Secondary organic aerosol and organic nitrogen yields from the nitrate radical (NO 3) oxidation of alpha-pinene from various RO 2 fates, Atmospheric Chemistry and Physics, 22, 1467-1482, 2022.

Han, S., and Jang, M.: Prediction of secondary organic aerosol from the multiphase reaction of gasoline vapor by using volatility–reactivity base lumping, Atmospheric Chemistry and Physics, 22, 625-639, 2022.

Jenkin, M., Wyche, K., Evans, C., Carr, T., Monks, P., Alfarra, M., Barley, M., McFiggans, G., Young, J., and Rickard, A.: Development and chamber evaluation of the MCM v3.2 degradation scheme for beta-caryophyllene, Atmospheric Chemistry and Physics, 12, 5275-5308, 10.5194/acp-12-5275-2012, 2012.

Jenkin, M., Young, J., and Rickard, A.: The MCM v3. 3.1 degradation scheme for isoprene, Atmospheric Chemistry and Physics, 15, 11433-11459, 2015.

Molteni, U., Simon, M., Heinritzi, M., Hoyle, C. R., Bernhammer, A.-K., Bianchi, F., Breitenlechner, M., Brilke, S., Dias, A., and Duplissy, J.: Formation of highly oxygenated organic molecules from α-pinene ozonolysis: chemical characteristics, mechanism, and kinetic model development, ACS Earth and Space Chemistry, 3, 873-883, 2019.

Paulson, S. E., Flagan, R. C., and Seinfeld, J. H.: Atmospheric photooxidation of isoprene part I: The hydroxyl radical and ground state atomic oxygen reactions, International Journal of Chemical Kinetics, 24, 79-101, 1992.

Roldin, P., Ehn, M., Kurtén, T., Olenius, T., Rissanen, M. P., Sarnela, N., Elm, J., Rantala, P., Hao, L., and Hyttinen, N.: The role of highly oxygenated organic molecules in the Boreal aerosol-cloud-climate system, Nature communications, 10, 1-15, 2019.

Saunders, S. M., Jenkin, M. E., Derwent, R., and Pilling, M.: Protocol for the development of the Master Chemical Mechanism, MCM v3 (Part A): tropospheric degradation of non-aromatic volatile organic compounds, Atmospheric Chemistry and Physics, 3, 161-180, 2003.

Zhao, D., Pullinen, I., Fuchs, H., Schrade, S., Wu, R., Acir, I.-H., Tillmann, R., Rohrer, F., Wildt, J., and Guo, Y.: Highly oxygenated organic molecule (HOM) formation in the isoprene oxidation by NO 3 radical, Atmospheric Chemistry and Physics, 21, 9681-9704, 2021.